J Mater Sci: Mater Med (2009) 20:2215–2222
DOI 10.1007/s10856-009-3793-2

Calcification capacity of porous pHEMA–TiO_2 composite hydrogels

Chao Li · Yu-Feng Zheng · Xia Lou

Received: 15 January 2009 / Accepted: 29 May 2009 / Published online: 11 June 2009

Abstract Many investigations have been attempted to promote calcification of synthetic polymers for applications as orthopaedic and dental implants. In this study, novel titanium dioxide (TiO_2) reinforced porous poly(2-hydroxyethyl methacrylate) (pHEMA) hydrogels were synthesized. Calcification capacity of the composite polymers was examined using light microscopy, scanning electron microscopy and Fourier transform infrared spectroscopy after incubation of the materials in a simulated body fluid up to 53 days. Mechanical strength, porosity and in vitro cytotoxicity were also investigated. Calcification capacity of porous pHEMA was significantly enhanced by the addition of TiO_2 particulates. Infiltration of calcium phosphate, up to 1000 μm, was observed. The diffusion capacity of calcium ions was affected by the porosity and the interconnectivity of pores in the hydrogel polymers which were influenced by the presence of TiO_2 and the monomer concentration. Cell viability tests indicated that porous hydrogels containing 7.5% TiO_2 were not toxic to 3T3 fibroblast cells. These results demonstrate that incorporating TiO_2 nanoparticulates can promote enhanced formation of calcium phosphate whilst maintaining the porosity and interconnectivity of the hydrogel polymers and would be very useful for the development of orthopaedic tissue engineering scaffolds.

C. Li · X. Lou (✉)
Department of Chemical Engineering & Nanochemistry Research Institute, Curtin University of Technology, Bentley, WA 6102, Australia
e-mail: x.lou@curtin.edu.au

Y.-F. Zheng · X. Lou
Centre for Biomedical Materials and Engineering, Harbin Engineering University, Harbin, China

1 Introduction

Poly(2-hydroxyethyl methacrylate) (pHEMA) hydrogels are well known for their successful use as vision correction devices, including contact lenses, intraocular lenses and cornea implants [1–4]. Extensive investigations on the use of pHEMA hydrogels as cardiovascular and breast implants have not been as successful. It has been generally accepted that calcification, the formation of calcium phosphate [CaP], on the surface and/or within the matrix of pHEMA, is one of the major drawbacks for its extended applications. This is particularly true for applications as breast implants [5]. Even for the contact ocular lenses, deposition of CaP on pHEMA is frequently reported and has been a major concern for the extended use of the lenses [6, 7]. It is unclear whether or not calcification of these materials is associated with the presence of blood components. However the physical properties of the materials, including their electric charges [8] and topographical and morphological properties [9], have been found to affect the nucleation and growth of calcium deposits in the materials. Up to now, calcification of pHEMA has been considered an adverse effect and a hindrance for its use as a prosthetic material. This has attracted numerous investigations aimed at understanding its intrinsic mechanism and preventing it from occurring [10].

On the other hand, many investigations have been attempted to promote calcification of synthetic biomaterials for applications in orthopaedic and dental surgery. It has been recognised that deposition of hydroxyapatite (HA) like CaP onto biomaterials surfaces can facilitate direct bonding to hard tissue which in turn provides a favourable procedure to mimic the bone environment through the promotion of osteointegration by osteoblast attachment and osteogenic differentiation [11]. Having considered both

facts that porous pHEMA has been successful in promoting tissue integration and biocolonisation in the medical implants [12, 13], and that calcium deposits on pHEMA have been identified as apatite like CaP by many researchers, it would be interesting to explore the possible applications of porous pHEMA as tissue scaffolds for orthopaedic and dental surgeries.

It is worth mentioning that in most of the aforementioned applications, pHEMA hydrogels are lightly crosslinked and are often produced by bulk polymerization, which results in transparent and homogeneous polymer networks that contain pores measured in nanometers, and are therefore classified as nonporous. Polymers of this type are ideally suited for applications in which a combination of optical clarity and limited diffusion characteristics is required. Porous pHEMA made in the presence of a large quantity of water is chemically identical to this analogue, but contains large pores ranging from several to several hundred micrometers. The formation of pores is a consequence of a phase separation during the polymerization process and the size and distribution of pores can be manipulated by altering the polymerization conditions including the monomer water ratio and crosslinking concentration [8, 14]. In comparison to the transparent homogenous pHEMA hydrogels, porous pHEMA has generated less interest until its applications as a key component of two ophthalmic implants [4, 5]. The large pores in the porous pHEMA play an important role in these implants. They allow the growth of cells and host tissues across the polymer-tissue interface and into the interconnected network of pores, therefore preventing extrusion of the implants that is the one of the most devastating post surgical complications. The interconnected network of pores is also a useful property which can be used in developing tissue scaffolds for tissue engineering applications and controlled drug delivery systems. On the other hand, TiO_2 particles have shown excellent capacity for inducing calcium deposition and osteoblast functions in polymers containing nano-sized titania inclusions [15, 16]. They have also demonstrated good compatibility with bone cells and tissues in many of these applications. It is foreseen that incorporating TiO_2 particles would enhance the calcification capacity of pHEMA hydrogels. To examine the effect of nanoparticulate TiO_2 on the calcification capacity of porous pHEMA, several porous pHEMA hydrogels were produced in the presence of TiO_2 nanoparticles. The mechanical strength and calcification capacity of these materials were examined. In vitro cytotoxicity of the produced composite hydrogel scaffolds were also assessed. The effects of TiO_2 content on the hydrogel porosity, calcification capacity and cytotoxicity are discussed.

2 Experimental

2.1 Materials

Ophthalmic grade 2-hydroxyethyl methacrylate (HEMA) and ethylene dimethacrylate (EDMA) were supplied by Bimax USA. TiO_2 nanoparticles (AEROXIDE® P 25, 99.5 wt%) were obtained from Degussa AG Germany. The average size of the particles was 21 nm. Ammonium persulphate (APS) and *N*,*N*,*N*′,*N*′-tetramethylethylenediamine (TEMED) were purchased from Sigma-Aldrich and used as initiators for polymerization. Simulated body fluid (SBF) was prepared according to an established method reported by Tanahashi et al. [17]. Ion strength was made to that equivalent to 1.5 times that in human blood plasma. All chemicals used for SBF preparation were analytical grade.

2.2 Synthesis of pHEMA–TiO_2 composite hydrogels

Six composite scaffolds (10HEMA–7.5TiO_2, 20HEMA–5TiO_2, 20HEMA–7.5TiO_2, 30HEMA–5TiO_2, 30HEMA–7.5TiO_2 and 40HEMA–7.5TiO_2) and two control hydrogels (20HEMA and 30HEMA, containing no TiO_2) were prepared following standard protocols. In brief, TiO_2 nanoparticles were dispersed in water using an ultrasonic bath. HEMA monomer, crosslinking agent (EDMA), and initiators (10 wt% APS solution and TEMED) were added subsequently using the formulation given in Table 1. The mixture was injected into a space between two glass plates separated with a silicon rubber gasket. Afterwards, the casting unit was kept at room temperature for 3 h followed by thermal curing at 60°C for 24 h. Upon completion of the polymerization, the hydrogel materials were removed from the glass plates and extracted with sufficient deionized water in order to remove residual chemicals and monomers. The extracted specimens were then kept in deionized water for further analysis.

2.3 Characterization of pHEMA–TiO_2 composite hydrogels

The porous structure of the hydrogel polymers was examined using scanning electron microscopy (SEM). The polymer density of all hydrogels was determined using a previously developed method and was used as a quantitative estimate of porosity. Tensile testing was carried out using a SINTECH® 200/M Material Testing Workstation (MTS Systems Corporation, USA) at a crosshead speed of 0.5 mm/s. Details of these measurements can be found in our previous work [18, 19].

The content of TiO_2 particles in each composite hydrogel was measured using gravimetric analysis (GA).

Table 1 Chemical composition and physical properties of pHEMA and pHEMA–TiO_2 hydrogels

Sample ID	TiO_2 (g)	HEMA (g)	Water (g)	EDMA (μl)	APS (10 wt%) (μl)	TEMED (μl)	Measured TiO_2 concentration *n* (%)	Polymer density (g/cm^3)
20HEMA	0	2.0	8.0	10	30	20	0	0.23
30HEMA	0	3.0	7.0	15	45	30	0	0.33
10HEMA–7.5TiO_2	0.075	1.0	9.0	5	15	10	7.8 ± 0.1	0.14
20HEMA–5TiO_2	0.1	2.0	8.0	10	30	20	3.4 ± 0.2	0.24
20HEMA–7.5TiO_2	0.15	2.0	8.0	10	30	20	6.8 ± 0.2	0.23
30HEMA–5TiO_2	0.15	3.0	7.0	15	45	30	3.7 ± 0.4	0.35
30HEMA–7.5TiO_2	0.225	3.0	7.0	15	45	30	6.7 ± 0.5	0.35
40HEMA–7.5TiO_2	0.3	4.0	6.0	18.9	60	40	7.0 ± 0.1	0.52

Three samples from each formulation were placed in a furnace at 450°C for complete decomposition. The samples were removed when they had reached a constant weight. The weights of the samples before and after decomposition were taken as W_1 and W_2, respectively. The weight percentage of TiO_2 in the composite hydrogels was calculated as $100 \times W_2/(W_1 - W_2)$. Three measurements were conducted for each specimen and the average weight percentage of TiO_2 was computed (Table 1).

2.4 Formation of calcium phosphate

SBF has proved to be very useful in examining the capacity of HA-like calcium phosphate formation [20]. In this study, five specimens of disk geometry (ca. 8 mm in diameter) were removed from each fully hydrated hydrogel polymer and kept in 10 ml SBF solution at 37 ± 1°C. The SBF solution was replaced with fresh solution weekly for up to 53 days. Samples were retrieved at 3, 14, 28, and 53 days, respectively. Thin sections were retrieved using a cryostat LEICA CM3050S. The formation of CaP was confirmed using Fourier transform infrared (FTIR) vibrational spectroscopy. The calcified samples were further examined by SEM and light microscopy (LM) after staining with a 2% Alizarin Red S solution.

2.5 FTIR, SEM and X-ray diffraction (XRD) analysis

FTIR examination was carried out using a Bruker IFS 66 with a resolution of 4 cm^{-1}. OPUS software was used for data analysis. The composite hydrogels were first freeze-dried and crashed into fine powder prior to the KBr disc preparation. Morphological analysis was conducted using a SEM (Zeiss 1555 VP FE-SEM and Philips XL30 SEM). The specimens were dried and coated with a thin layer of carbon using a Speedivac coating unit (model 12E6/1167, Edwards High Vacuum LTD) prior to the SEM measurements. XRD measurements were performed on a Siemens D-500 powder diffractometer using Cu Kα radiation. It was operated at 40 kV/30 mA. The scanning was carried out from 20° to 70° with a step size of 0.02° and a count time of 1.5 s/step. To minimize non-desirable scattering signals, a low background specimen-holder made of silicon single crystal was utilized in all measurements.

2.6 In vitro cytotoxicity assay

The 3-(4,5-dimethylthiazol-2-yl)-2,5-diphenyltetrazolium bromide (MTT) assay was used to examine the cytotoxicity of the prepared materials. 3T3 fibroblast cells were cultured in a Dulbecco's modified Eagle's medium (DMEM) containing 10% fetal calf serum (FCS) and 1% penicillin/streptomycin (Gibco, USA) at 37°C in a humidified 5% CO_2 incubator. Hydrogel disks (10 mm in diameter, 1.5 mm in thickness) were steam sterilized (121°C, 15 min) prior to the pre-culture with DMEM media in 24-well cell culture plates for 2 h. 150 μl of cell suspension with a density of 8.5×10^4 cells/ml was placed onto each of the disks after the pre-culture media was aspirated. A quantity of 200 ml fresh media was carefully added after 1 h. At the desired times (day 1 and day 3), 30 μl fresh MTT solution (5 mg/ml in PBS) was added to each well and the culture plates were incubated for 6 h. The formed purple formazan was dissolved with 200 μl sodium dodecyl sulfate solution in hydrochloric acid (pH 4.7). The culture plates were kept in the incubator overnight. Optical density of each well was measured after the scaffolds were removed from the culture plate with a spectrophotometer (Beckman, USA) at 570 nm with background subtraction at 650 nm. Readings of four disks were taken for each formulation.

Statistical analysis was performed between the groups. Mean ± standard deviation and the *P* value were calculated using one-way ANOVA with SPSS software and Turkey test. *P* values <0.05 were considered statistically significant.

3 Results and discussion

3.1 Synthesis and physical properties of pHEMA–TiO_2 hydrogels

Eight porous hydrogel polymers were prepared including 20HEMA, 30HEMA, 10HEMA–7.5TiO_2, 20HEMA–5TiO_2, 20HEMA–7.5TiO_2, 30HEMA–5TiO_2, 30HEMA–7.5TiO_2 and 40HEMA–7.5TiO_2. All samples appeared translucent or opaque due to the presence of pores. Sample codes and the chemical compositions of these materials are listed in Table 1 (10, 20, 30 and 40 denote the percentage concentrations of HEMA in relation to the total quantity of HEMA and water used in the monomer mixture; 5 and 7.5 represent the initial percentage concentrations of TiO_2 based on the mass of HEMA). Polymer density and the measured TiO_2 concentration in each hydrogel polymer are also summarized in Table 1.

A decrease in polymer density was observed in hydrogels containing decreased HEMA concentration, indicating an increase in the number and/or size of pores caused by the increased phase separation of the polymers from water phase due to the thermodynamic effect. This change was also reflected in the morphology of samples revealed by SEM (Fig. 1). Little change in polymer density has been observed when TiO_2 was added to the hydrogel polymers (0.23, 0.24, 0.23 for 20HEMA, 20HEMA–5TiO_2 and 20HEMA–7.5TiO_2, respectively, and 0.33, 0.35, 0.35 for 30HEMA, 30HEMA–5TiO_2 and 30HEMA–7.5TiO_2, respectively) although some variations in morphology were apparent (Fig. 1a vs. b, c vs. d). This indicated that the entrapment of TiO_2 nanoparticulates in the hydrogel polymer has resulted in some disturbance in the formation of microstructures, but the effect was not sufficient to affect the value of polymer density.

Gravimetric analysis indicated that the TiO_2 content was similar to the initial concentration when 7.5% nanoparticles were used. The entrapment efficiency of TiO_2 particles was much lower at 5% initial particle concentration leading to a content of TiO_2 below 4% (Table 1). Uniformly distributed TiO_2 nanoparticles with some aggregations were demonstrated in all polymer matrices (Fig. 2).

Tensile modulus and strength of the composite hydrogels increased dramatically with the increase in HEMA/water ratio in the monomer mixture. The increases were caused by the decrease of porosity and increased polymer density of the hydrogel matrix (Fig. 3). There was a slight increase in tensile strength in most composite hydrogels after the addition of TiO_2 particulates. The change became more significant in hydrogels containing a high HEMA/water ratio such as 40HEMA–7.5TiO_2 due to the less porous structure. Change in tensile modulus by TiO_2 was insignificant and without an apparent pattern. This was probably due to the particularly small size and generally low concentration of TiO_2 particulates. A drastic reduction of tensile strength was observed when comparing

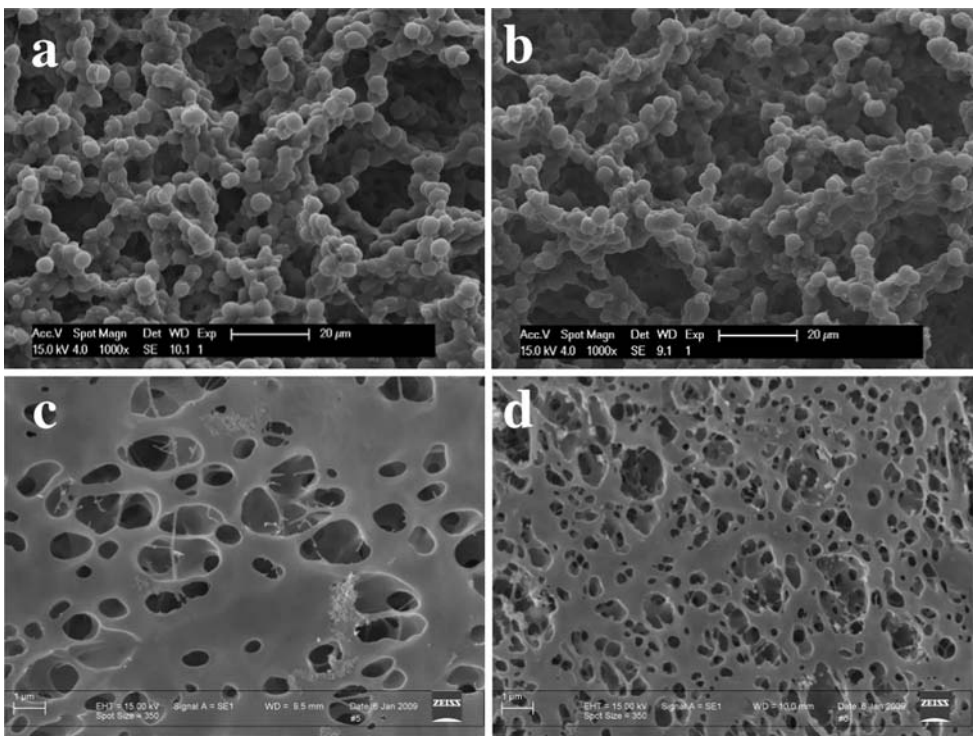

Fig. 1 SEM micrographs of 20HEMA (**a**), 20HEMA–5TiO_2 (**b**), 30HEMA (**c**) and 30HEMA–5TiO_2 (**d**) showing the effect of HEMA/water ratio and TiO_2 concentration on the porosity of hydrogels

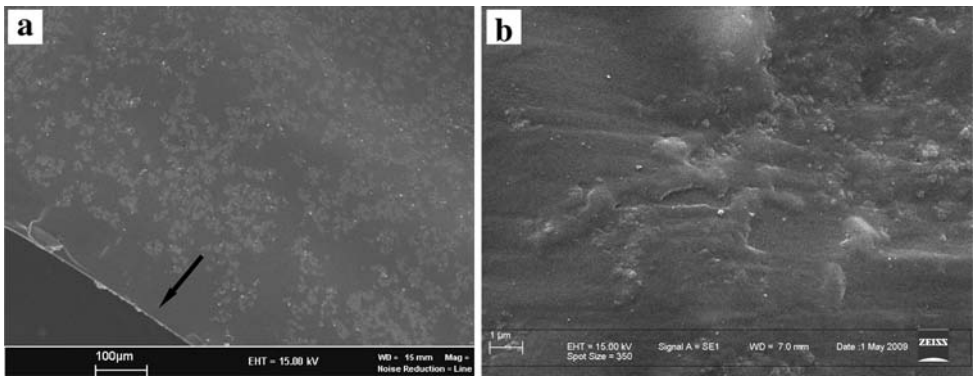

Fig. 2 SEM micrographs of 40HEMA–7.5TiO_2 showing distribution of TiO_2 particles within hydrogel matrix. *Arrow* indicates the top edge of the sample

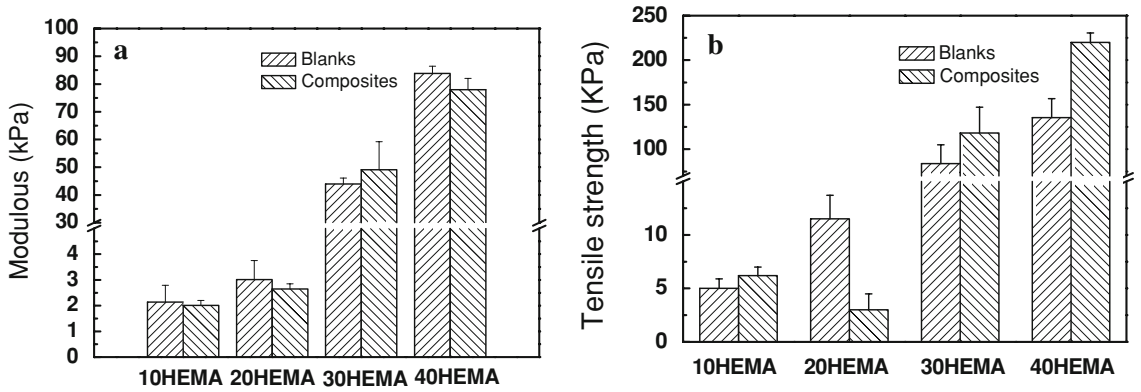

Fig. 3 Tensile modulus (**a**) and strength (**b**) of the porous pHEMA–TiO_2 hydrogel materials

20HEMA–TiO_2 with its control polymer 20HEMA (Fig. 3b). Repeated testing on the same hydrogel and those produced in different batches yielded similar results.

3.2 Calcification capacity of pHEMA–TiO_2 composite hydrogels

Formation of CaP on the hydrogel composites after incubation in SBF was confirmed by FTIR (Fig. 4a) which showed strong absorbance at 564 and 603 cm^{-1}, and between 1000 and 1200 cm^{-1}, respectively, due to the asymmetric bending and stretching modes of the phosphate group. In comparison to the FTIR spectrum of the same material before incubation in SBF (Fig. 4b), there was also a slight change at 964 cm^{-1}, attributed to the symmetric stretching mode of the phosphate group.

The formation of CaP crystals was also revealed by SEM and LM following Alizarin staining of the specimens

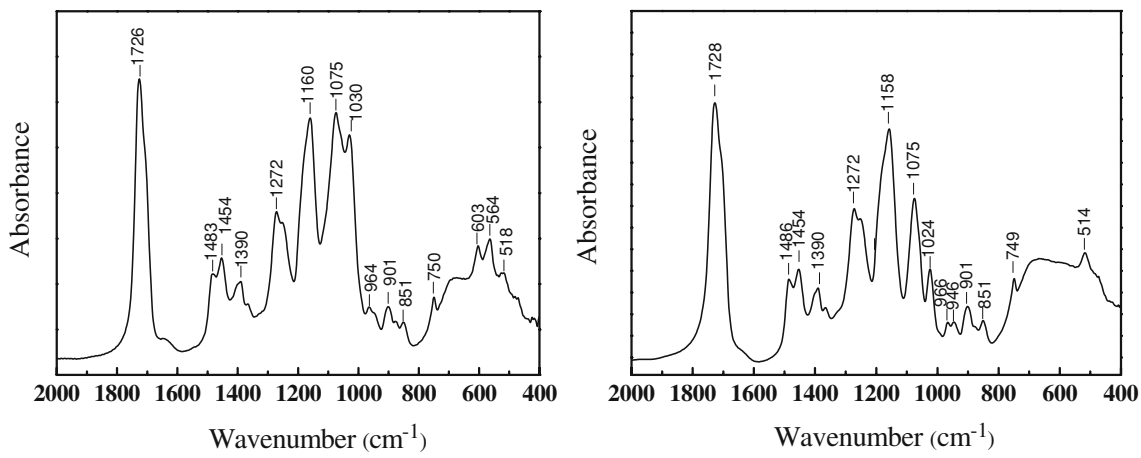

Fig. 4 FTIR of 10HEMA–7.5TiO_2 after (**a**) and before calcification (**b**) indicating the formation of the calcium phosphate

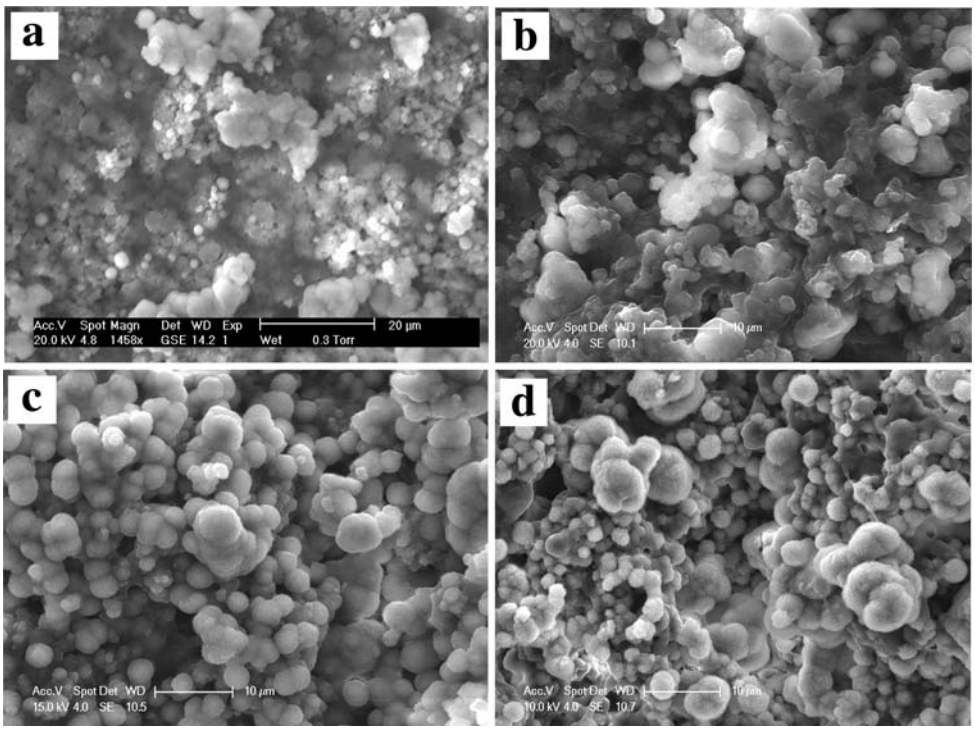

Fig. 5 SEM micrographs of 20HEMA–7.5TiO_2 composite scaffold after incubation in SBF for 3 days (**a**), 14 days (**b**), 28 days (**c**) and 53 days (**d**)

(Figs. 5, 7). The appearance of calcium phosphate deposits on the composite hydrogel 20HEMA–7.5TiO_2 was observed at as early as day 3 (Fig. 5a). Further examination of the incubated specimens at day 14, 28 and 53 (Fig. 5b–d) showed that the density of calcium phosphate deposits, in singular spherical or aggregated forms, increased with increasing incubation time. At day 28, the surface of the TiO_2 containing hydrogel became fully covered with calcium phosphate. There appeared finer particles on the hydrogel surface at day 53 which is probably due to the reduction of ion concentrations in the SBF after 28 days (no more refreshing with SBF). On the other hand, calcium phosphate was barely observable on the control 20HEMA (containing no TiO_2) until day 28 (Fig. 6). This indicates that the formation of calcium phosphate was enhanced by TiO_2 particles.

The formed Ca–P on various hydrogel materials after 3–4 weeks incubation was stained with Alizarin red [8]. The optical micrographs of the stained samples were shown in Fig. 7. Significant enhancement in calcification capacity was demonstrated in all pHEMA–TiO_2 hydrogels (Fig. 7b–f). Little Ca–P deposit was found in 20HEMA (Fig. 7a). Infiltration of calcium up to 800–1000 μm was observed in 10HEMA–7.5TiO_2, 20HEMA–5TiO_2 and

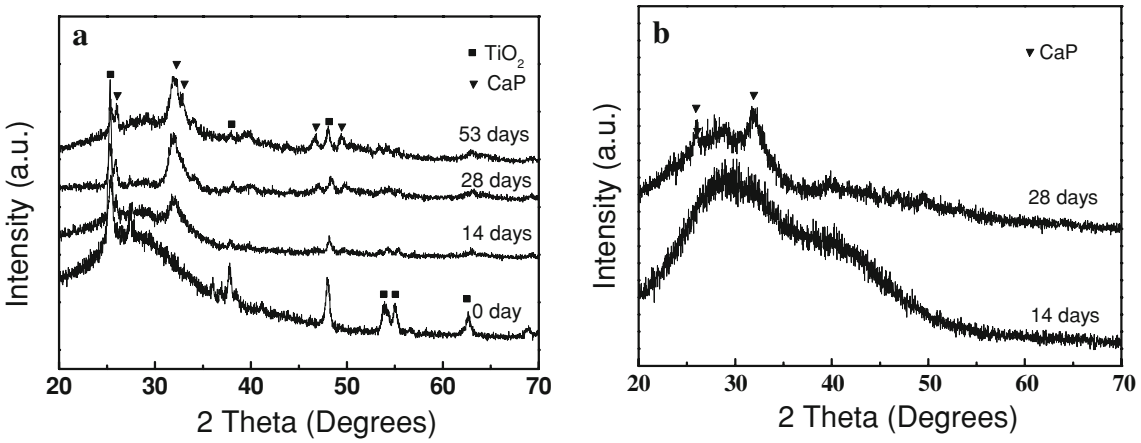

Fig. 6 XRD of 20HEMA–7.5TiO_2 (**a**) and 20HEMA (**b**) after incubation in SBF for various periods of time. No significant calcium phosphate was formed in 20HEMA until 28 days

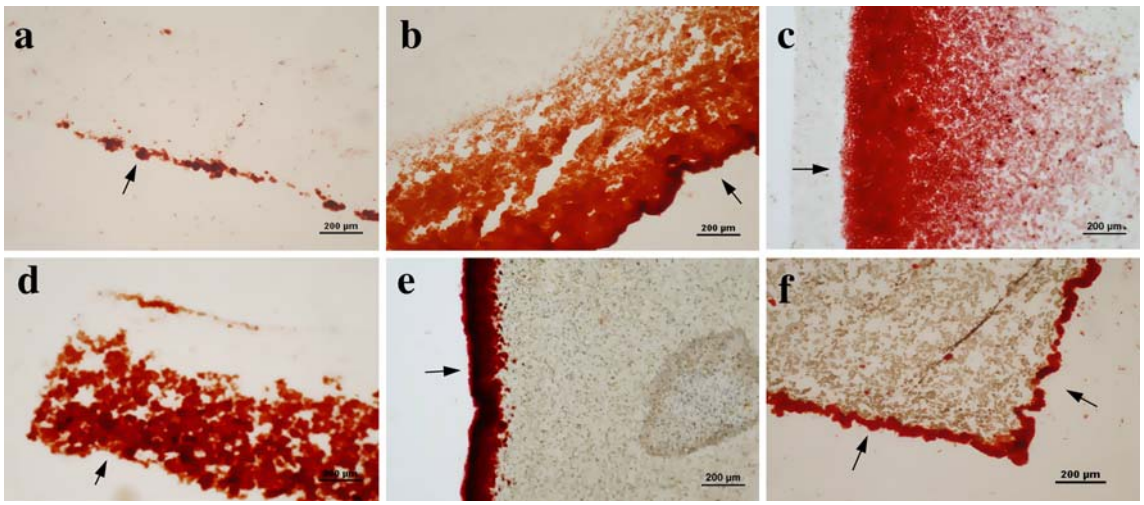

Fig. 7 Alizarin staining of 20HEMA (**a**), 10HEMA–7.5TiO_2 (**b**), 20HEMA–5TiO_2 (**c**), 20HEMA–7.5TiO_2 (**d**), 30HEMA–5TiO_2 (**e**) and 40HEMA–7.5TiO_2 (**f**) after 28 days incubation in SBF, indicating the effect of porosity on calcification capacity of the hydrogels. Arrows indicate the edges of hydrogels exposed to SBF solutions

20HEMA–7.5TiO_2 (Fig. 7b–d). Diffusion of calcium ions was reduced to about 200 μm in 30HEMA–5TiO_2 and further reduced to less than 100 μm in 40HEMA–7.5TiO_2 (Fig. 7e, f). Whilst the rapid infiltration of calcium was due to the change in size and connectivity of pores of the materials, the increased intensity of Ca–P in TiO_2 containing hydrogels was largely due to the incorporation of TiO_2 nanoparticles.

3.3 Cytotoxicity examination

3T3 fibroblast cells were used to examine the in vitro cytotoxicity of all composite hydrogels using the MTT assay, a commonly used colorimetric method for cell viability determination that is based on the selective ability of viable cells to reduce MTT into purple formazan upon intact metabolic activities [21]. 20HEMA hydrogel is an America Food and Drug Administration (FDA) approved material for ophthalmic implants [3, 22] and therefore used as a control material. Figure 8 shows the 3T3 fibroblast cell viability as a function of incubation time. There was no significant difference among the materials after 1 day incubation. Apparent cell growth was demonstrated in all materials from day 1 to day 3. There was no difference between the cell viability of the control hydrogels and that of the composite hydrogels, 10HEMA–TiO_2 and 20HEMA–TiO_2. A slight reduction of cell growth on 40HEMA–TiO_2 and a more significant reduction on 30HEMA–TiO_2 were observed that is probably due to the smooth surface features of these two materials that are less preferable to the anchorage dependent fibroblast cells (Fig. 8).

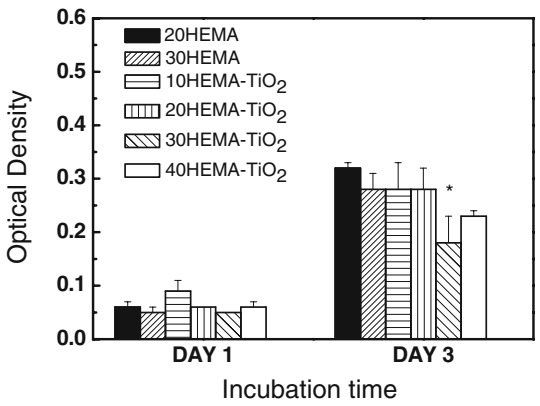

Fig. 8 In vitro cytotoxicity examination on pHEMA and its composite hydrogels containing 7.5% TiO_2 by MTT assay. The obtained OD values are proportional to the numbers of the cells. * indicates significant difference in cytotoxicity when compared to 20pHEMA and 30pHEMA

4 Conclusions

This study has demonstrated that the calcification capacity of porous pHEMA hydrogels can be significantly enhanced using TiO_2 nanoparticles. Alternation of porosity and hydrogel composition can also improve the strength and the infiltration capacity of the calcium phosphate deposits. At low HEMA concentrations, the composite hydrogels contain more pores and better surface properties and are favorable to both the formation of calcium phosphate and cell growth. At high HEMA concentrations, the addition of TiO_2 has a larger impact on the enhancement of mechanical strength of the hydrogel polymers than on the

calcification capacity. The choice of the application for these materials should be based on whether it is used for soft tissue or hard tissue repairing.

Acknowledgement This work was supported by the Australian Research Council Discovery Project Grant (DP0557148). We thank Dr Choo-May Lai of Lions Eye Institute Perth for technical assistance in cell culture experiments.

References

1. Refojo MF. Polymers in ophthalmology: an overview. In: Williams DF, editor. Biocompatibility in clinical practice, vol. II. Boca Raton, FL: CRC Press; 1982. p. 3.
2. Mack EJ, Okano T, Kim SW. Biomedical applications of poly (2-hydroxyethyl methacrylate) and its copolymers. In: Peppas NA, editor. Hydrogels in medicine and pharmacy, vol. II. Boca Raton, FL: CRC Press; 1987. p. 65.
3. Hick CR, Crawford G, Chirla TV, Wiffen S, Vijayasekeran S, Lou X, et al. Development and clinical assessment of an artificial cornea. Prog Retin Eye Res. 2000;19:149–70. doi:10.1016/S1350-9462(99)00013-0.
4. Hicks CR, Morrison D, Lou X, Crawford GJ, Gadjatsy A, Constable IJ. Orbit implants: potential new directions. Expert Rev Med Devices. 2006;3:805–15. doi:10.1586/17434440.3.6.805.
5. Calnan JS, Pflug JJ, Chhabra AS, Raghupati N. Clinical and experimental studies of polyhydroxyethyl methacrylate gel ("Hydron") for reconstructive surgery. Br J Plast Surg. 1971; 24:113–24. doi:10.1016/S0007-1226(71)80029-2.
6. Tripathi RC, Tripathi BJ, Silverman RA, Rao GN. Contact lens deposits and spoilage: identification and management. Int Ophthalmol Clin. 1991;31:91–120. doi:10.1097/00004397-199103120-00012.
7. Bowers RWJ, Tighe BJ. Studies in the ocular compatibility of hydrogels: a review of the clinical manifestations of spoilation. Biomaterials. 1987;8:83–8. doi:10.1016/0142-9612(87)90094-9.
8. Lou X, Vijayasekaran S, Sugiharti R, Robertson T. Morphological and topographic effect on calcification tendency of pHEMA hydrogels. Biomaterials. 2005;26:5808–17. doi:10.1016/j.biomaterials.2005.02.034.
9. Chirila TV, Zainuddin. Calcification of synthetic polymers functionalized with negatively ionizable groups: a critical review. React Funct Polym. 2007;67:165–72. doi:10.1016/j.reactfunctpolym.2006.10.008.
10. Chirila TV, Zainuddin, Hill DJT, Whittaker AK, Kemp A. Effect of phosphate functional groups on the calcification capacity of acrylic hydrogels. Acta Biomater. 2007;3:95–102. doi:10.1016/j.actbio.2006.07.011.
11. Yokogawa Y, Reyes JP, Mucalo MR, Toriyama M, Kawamoto Y, Suzuki T, et al. Growth of calcium phosphate on phosphorylated chitin fibres. J Mater Sci: Mater Med. 1997;8:407–12. doi:10.1023/A:1018549404092.
12. Crawford GJ, Hicks CR, Lou X, Vijayasekaran S, Tan D, Chirila TV, et al. Ophthalmology. 2002;109:883. doi:10.1016/S0161-6420(02)00958-2.
13. Chirila TV, Hicks CR, Dalton PD, Vijayasekaran S, Lou X, Hong Y, et al. Artificial cornea. Prog Polym Sci. 1998;23:447–73. doi:10.1016/S0079-6700(97)00036-1.
14. Chirila TV, Constable IJ, Crawford GJ, Vijayasekaran S, Thompson DE, Chen YC, et al. Poly(2-hydroxyethyl methacrylate) sponges as implant materials: *in vivo* and *in vitro* evaluation of cellular invasion. Biomaterials. 1993;14:26–38. doi:10.1016/0142-9612(93)90072-A.
15. Webster TJ, Savaiano JK. Altered responses of chondrocytes to nanophase PLGA/nanophase titania composites. Biomaterials. 2004;25:1205–13. doi:10.1016/j.biomaterials.2003.08.012.
16. Liu HN, Slamovich EB, Webster TJ. Increased osteoblast functions among nanophase titania/poly(lactide-co-glycolide) composites of the highest nanometer surface roughness. J Biomed Mater Res A. 2006;78A:798–807. doi:10.1002/jbm.a.30734.
17. Tanahashi M, Yao T, Kokubo T, Minoda M, Miyamoto T, Nakamura T, et al. Apatite coating on organic polymers by a biomimetic process. J Am Ceram Soc. 1994;77:2805–8. doi:10.1111/j.1151-2916.1994.tb04508.x.
18. Lou X, Munro S, Wang S. Drug release characteristics of phase separation pHEMA sponge materials. Biomaterials. 2004;25:5071–80. doi:10.1016/j.biomaterials.2004.01.058.
19. Lou X, Wang S, Tan SY. Mathematics-aided quantitative analysis of diffusion characteristics of pHEMA sponge hydrogels. Asia-Pac J Chem Eng. 2007;2:609–17. doi:10.1002/apj.62.
20. Kokubo T, Takadama H. How useful is SBF in predicting *in vivo* bone bioactivity? Biomaterials. 2007;27:2907–15. doi:10.1016/j.biomaterials.2006.01.017.
21. Mosmann T. Rapid colorimetric assay for cellular growth and survival: application to proliferation and cytotoxicity assays. J Immunol Methods. 1983;65:55–63. doi:10.1016/0022-1759(83)90303-4.
22. Hicks CR, Crawford GJ, Lou X, Tan DT, Snibson GR, Sutton G, et al. Corneal replacement using a synthetic hydrogel cornea, AlphaCorT: device, preliminary outcomes and complications. Eye. 2003;17:385–92. doi:10.1038/sj.eye.6700333.